Simulation of Fluid Flow and Heat Transfer in Inclined Cavity using Lattice Boltzmann Method

Arash Karimipour, A. Hossein Nezhad, E. Shirani, A. Safaei

Abstract—In this paper, Lattice Boltzmann Method (LBM) is used to study laminar flow with mixed convection heat transfer inside a two-dimensional inclined lid-driven rectangular cavity with aspect ratio *AR = 3*. Bottom wall of the cavity is maintained at lower temperature than the top lid, and its vertical walls are assumed insulated. Top lid motion results in fluid motion inside the cavity. Inclination of the cavity causes horizontal and vertical components of velocity to be affected by buoyancy force. To include this effect, calculation procedure of macroscopic properties by LBM is changed and collision term of Boltzmann equation is modified. A computer program is developed to simulate this problem using BGK model of lattice Boltzmann method. The effects of the variations of Richardson number and inclination angle on the thermal and flow behavior of the fluid inside the cavity are investigated. The results are presented as velocity and temperature profiles, stream function contours and isotherms. It is concluded that LBM has good potential to simulate mixed convection heat transfer problems.

Keywords—gravity, inclined lid driven cavity, lattice Boltzmann method, mixed convection.

I. INTRODUCTION

THE lattice Boltzmann Equation (LBE) is a minimal form of the Boltzmann kinetic equation and has gained much attention for its ability to simulate fluid flows, and for its potential advantages over conventional numerical solution of the Navier–Stokes (NS) equations. The key advantages of LBE are: (1) suitability for parallel computations, (2) absence of the need to solve the time-consuming Poisson equation for pressure, and (3) ease with which multiphase flows, complex geometries and interfacial flows may be treated [1, 2]. More details about LBE may be found in Refs. [3] to [8].

The lattice Boltzmann BGK (LBGK) method is a new numerical scheme for simulating viscous compressible flows in the subsonic regime. Guo et al [9] designed a LBGK model to simulate incompressible flows.

Some researchers have used lattice Boltzmann method to investigate fluid flow inside a cavity. Hou et al [10] used lattice Boltzmann BGK model (LBGK) to solve viscous flows in square two-dimensional cavity driven by shear from a moving wall for Reynolds numbers up to 10,000. They concluded that boundary conditions, lattice size and compressibility effects are important when the method is applied to other problems.Wu and Shao [11] simulated the

hydrodynamics of a two-dimensional near-incompressible steady lid-driven cavity flows *(Re = 100 – 7,500)* using multi-relaxation-time (MRT) model in the parallel lattice Boltzmann BGK Bhatnager–Gross–Krook method (LBGK). Having studied hydrodynamics of fluid flows using LBE method, researchers tried to use it to model thermo-hydrodynamics of fluid flows. He et al [12] proposed a thermal model for the lattice Boltzmann method. They claimed that it greatly improved the previous LBE thermal models. They introduced a new variable *g*, denoting the internal energy density distribution function, to simulate thermal behavior of fluid flows. Eggels and Somers [13] incorporated convective and diffusive scalar transport into the lattice Boltzmann discretization scheme to solve steady flow in a square cavity with heated and cooled side walls and descried the flow in the thin vertical boundary layers. They compared their results in detail with numerical results obtained using different numerical techniques.

Following previous efforts, researchers decided to investigate the capabilities of lattice Boltzmann method to solve free convections inside the cavities at high *Ra*. Dixit and Babu in 2004 [14] simulated high Rayleigh numbers natural convection in a square cavity using LBM. Barrios et al [15] used the lattice Boltzmann equation method in two dimensions to solve natural convective flow in an open cavity which the lower part of one of the vertical walls was conductive and its upper part and all other walls were adiabatic. They validated the results obtained from LBM with related experimental results.

Kao and Yang [16] employed a simple thermal LB model with the Boussinesq approximation to simulate the oscillatory flows of the secondary instability in 2D Rayleigh– Benard convection. Convection heat transfer in cavities has already been considered extensively, because of its wide applications in manufacturing of solar collectors and heat exchangers, or designing of cooling systems of electronic devices. Among them, mixed convection in a cavity with moving top lid has attracted more attention to be investigated.Most investigations have already been dedicated to horizontal cavities, in which gravitational acceleration is parallel to their sidewalls. However, in many cases it is necessary to use inclined cavities, in which, according to inclination angle of the cavities, the shear stress applied by lid on the flow increases or decreases the buoyancy force, hence, influence flow and thermal behavior of the fluid inside the cavity. Therefore, it is necessary to investigate the effect of the inclination angle on the flow and heat transfer in these cavities.

A few investigations of forced convection in a horizontal cavity with moving lid, using LBM, are found in the literature, but to the authors' knowledge, mixed convection in an inclined cavity with moving top lid has not been investigated

[1] PhD candidate; Islamic Azad University, NajafAbad Branch, Iran; (corresponding author; e-mail: arash.karimipour@pmc.iaun.ac.ir and arashkarimipour@gmail.com).
[2] Assistant professor; Department of Mechanical Engineering, University of Sistan and Baluchestan, Zahedan, Iran; (e-mail: Nezhadd@hamoon.usb.ac.ir)
[3] Professor; Department of Mechanical Engineering, Isfahan University of Technology, Isfahan, Iran; (e-mail: eshirani@ictp.it)
[4] MS, Islamic Azad University, NajafAbad Branch, Iran; (e-mail: abbas_safaei83@yahoo.com)

yet by this method. Therefore, in this paper, using LBM, laminar mixed convection in a two-dimensional rectangular inclined cavity with moving top lid, according to its importance, is investigated numerically, including the effects of the variations of Ri and inclination angle on fluid flow and heat transfer.

II. MATHEMATICAL FORMULATION

A. Problem Statement

In this paper, laminar mixed convection of a fluid inside a rectangular cavity with moving top lid and aspect ratio $AR = L / H = 3$, in which L and H are shown in Fig. 1, is studied numerically using lattice Boltzmann method. Temperature of the bottom wall is less than that of the top lid, and vertical walls are assumed insulated. Top lid moves with constant velocity U_0, and thus generates fluid flow inside the cavity. Using lattice Boltzmann BGK and internal energy density distribution models, a computer program is developed to simulate fluid flow and heat transfer of an incompressible fluid inside the cavity. In this method, hydrodynamic and thermal macroscopic parameters of fluid flow are calculated using density distribution function, f, and internal energy density distribution function, g, respectively. In the following sections, $Pr = 0.7$ and $Re = 200$ are assumed, and then the effects of the variations of Ri $(Ri = Gr / Re^2 = 0.1, 1, 10)$ and inclination angle $(\gamma = 0°$ to $90°)$ on fluid flow and heat transfer are studied.

Inclination of the cavity causes horizontal and vertical components of velocity to be affected by buoyancy force, leading to the changing of the calculation procedure of macroscopic properties by LBM and the modifying of the collision term of Boltzmann equation.

B. Lattice Boltzmann Method

The evolution of the single-particle density distribution in a fluid system obeys the Boltzmann equation, [12]:

$$\partial_t f + (\xi.\nabla)f = \Omega(f) \quad (1)$$

where f is the density distribution function, ξ is the microscopic velocity, and Ω is the collision term. Since collision term in lattice Boltzmann equation is very complex, for practical calculations, it is simplified and replaced with single relaxation time BGK model [16, 17] as follows:

$$\partial_t f + (\xi.\nabla)f = -\frac{f - f^e}{\tau_f} \quad (2)$$

where τ_f is the relaxation time and f^e is the Maxwell–Boltzmann equilibrium distribution defined as

$$f^e = \frac{\rho}{(2\pi RT)^{D/2}} exp\left[-\frac{(\xi - u)^2}{2RT}\right] \quad (3)$$

Here R is the gas constant and D is a dimension. f carries mass and momentum according to the standard kinetic moments:

$$\rho(x,t) = \int f(x,\xi,t)d\xi \quad (4)$$

$$\rho(x,t)u(x,t) = \int \xi f(x,\xi,t)d\xi \quad (5)$$

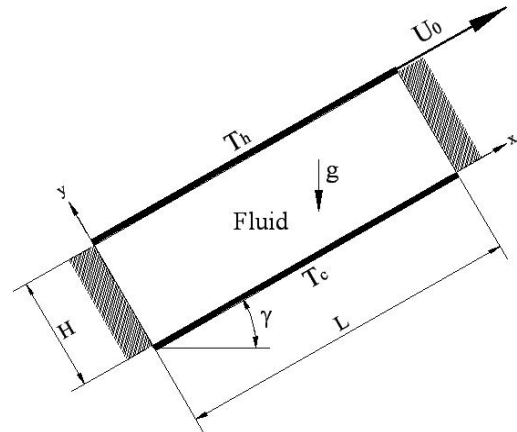where ρ is density and u is fluid velocity.

Fig. 1 Geometry and boundary conditions of the inclined cavity

C. Thermal LBM

In thermal energy distribution model, LBE with double populations is used [12, 24] that is in addition to f, a new function named internal energy density distribution function, g, is used to simulate fluid heat transfer and macroscopic properties such as density and velocity are calculated using f, as stated in Eqs. (4) and (5), while temperature and heat flux is calculated using internal energy density distribution function, g, as stated in Eqs. (6) and (7).

$$\rho e(x,t) = \int g(x,\xi,t)d\xi \quad (6)$$

$$q(x,t) = \int v'g(x,\xi,t)d\xi \quad (7)$$

$e = DRT / 2$ is the internal energy and $v' = \xi - u$ is the molecular peculiar speed relative to the flow speed. For real gas, the following relationship must hold:

$$g(x,\xi,t) = 0.5|v'|^2 f(x,\xi,t) \quad (8)$$

More specifically [2]:

$$\partial_t g + (\xi.\nabla)g = 0.5|v'|^2 \Omega(f) - f(\xi - u) \times [\partial_t u + (\xi.\nabla)u] \quad (9)$$

where $\Omega(f)$ is the collision operator and the viscous heating term can be defined as:

$$-f(\xi - u).[\partial_t u + (\xi.\nabla)u] = -fZ \quad (10)$$

Using BGK model and single relaxation time and local equilibrium, the collision term is defined as follows:

$$0.5|v'|^2 \Omega(f) = \Omega(g) = -\frac{g - g^e}{\tau_g} \quad (11)$$

$$g^e = \frac{\rho(\xi - u)^2}{2(2\pi RT)^{D/2}} exp\left[-\frac{(\xi - u)^2}{2RT}\right] \quad (12)$$

D. Discretization of Thermal and Hydrodynamic LBM

In order to avoid the implicitness of the scheme, new discrete distribution functions $\tilde{f}_i$ and $\tilde{g}_i$ are introduced as [12]:

$$\tilde{f}_i = f_i + \frac{dt}{2\tau_f}(f_i - f_i^e) \tag{13}$$

$$\tilde{g}_i = g_i + \frac{dt}{2\tau_g}(g_i - g_i^e) + \frac{dt}{2}f_i Z_i \tag{14}$$

$$Z_i = (c_i - u).D_i u \text{ and } D_i = \partial_t + c_i.\nabla \tag{15}$$

The term Z_i represents the effects of viscous heating. Details about discretization of the microscopic velocity space using Gaussian-Hermite quadrature, for satisfying continuity, momentum and Navier-Stokes equations, can be found in Refs [12, 18, 19]. $\tilde{f}_i$ and $\tilde{g}_i$ obey a set of lattice BGK equations in the form:

$$\tilde{f}_i(x + c_i dt, t + dt) - \tilde{f}_i(x,t) =$$
$$-\frac{dt}{\tau_f + 0.5dt}\left[\tilde{f}_i - f_i^e\right] \tag{16}$$

$$\tilde{g}_i(x + c_i dt, t + dt) - \tilde{g}_i(x,t) =$$
$$-\frac{dt}{\tau_g + 0.5dt}\left[\tilde{g}_i - g_i^e\right] - \frac{\tau_g dt}{\tau_g + 0.5dt}f_i Z_i \tag{17}$$

where τ_f and τ_g are relaxations times and f_i^e and g_i^e are the equilibrium distribution functions. Throughout of this work, 9-Bit square lattice [2], as shown in Fig. 2, is used. The discrete particle lattice speed is:

$$c_i = \left(\cos\frac{i-1}{2}\pi, \sin\frac{i-1}{2}\pi\right)c, \ i = 1,2,3,4$$

$$c_i = \sqrt{2}\left(\cos\left[\frac{(i-5)}{2}\pi + \frac{\pi}{4}\right], \sin\left[\frac{(i-5)}{2}\pi + \frac{\pi}{4}\right]\right)c, \ i = 5,6,7,8 \tag{18}$$

$$c_0 = (0,0)$$

The equilibrium density distributions are defined as [2]:

$$f_i^e = \omega_i \rho\left[1 + \frac{3c_i \cdot u}{c^2} + \frac{9(c_i \cdot u)^2}{2c^4} - \frac{3(u^2 + v^2)}{2c^2}\right] \tag{19}$$

$$g_0^e = -\omega_0\left[\frac{3\rho e}{2}\frac{u^2 + v^2}{c^2}\right] \tag{20}$$

$$g_{1,2,3,4}^e = \omega_1 \rho e \times$$
$$\left[1.5 + 1.5\frac{c_i \cdot u}{c^2} + 4.5\frac{(c_i \cdot u)^2}{c^4} - 1.5\frac{u^2 + v^2}{c^2}\right] \tag{21}$$

$$g_{5,6,7,8}^e = \omega_2 \rho e \times$$
$$\left[3 + 6\frac{c_i \cdot u}{c^2} + 4.5\frac{(c_i \cdot u)^2}{c^4} - 1.5\frac{u^2 + v^2}{c^2}\right] \tag{22}$$

where $u = (u, v)$ and $\rho e = \rho RT$ (in 2 dimensional geometry). The weights of the different populations are as $\omega_0 = 4/9$ and $\omega_i = 1/9, i = 1, 2, 3, 4$ and $\omega_i = 1/36, i = 5, 6, 7, 8$.

Finally, using $\tilde{f}_i$ and $\tilde{g}_i$, hydrodynamic and thermal variables are calculated as follows [2]:

$$\rho = \sum_i f_i, \ \rho e = \sum_i g_i, \ \rho u = \sum_i c_i f_i,$$
$$q = \sum_i (c_i - u)g_i \tag{23}$$

$$\sum_i c_i g_i^e = \rho e u, \ \sum_i g_i^e = \rho e, \ \rho = \sum_i \tilde{f}_i,$$
$$\rho e = \sum_i \tilde{g}_i - \frac{dt}{2}\sum_i f_i Z_i, \ \rho u = \sum_i c_i \tilde{f}_i \tag{24}$$

$$q = \left(\sum_i c_i \tilde{g}_i - \rho e u - \frac{dt}{2}\sum_i c_i f_i Z_i\right)\frac{\tau_g}{\tau_g + 0.5dt} \tag{25}$$

$$c^2 = 3R\overline{T} \tag{26}$$

The kinematic viscosity and the thermal diffusivity in the two-dimensional geometry are given by [12]:

$$\upsilon = \tau_f R\overline{T}, \quad \alpha = 2\tau_g R\overline{T} \tag{27}$$

III. Effects of Gravity and Lid Motion

In this problem shear stress applied by moving lid on the fluid layers results in fluid motion, thus creating suitable temperature gradient that enhances buoyancy forces. Therefore, mixed convection is produced in the fluid confined in the cavity. To calculate buoyancy forces, Boussinesq approximation is used and density is written as $\rho = \overline{\rho}\left[1 - \beta(T - \overline{T})\right]$, in which β is volumetric expansion coefficient, $\overline{\rho}$ is average density and $\overline{T}$ is average temperature. One of the main parameters controlling natural convection flows is Rayleigh number defined as $Ra = \beta g \Delta T H^3 Pr / \upsilon^2$ in which ΔT is temperature difference between bottom wall and top lid of the cavity, and Pr denotes Prandtl number defined as $Pr = \upsilon / \alpha$. In order to simulate the mixed convection of nearly incompressible flows, buoyancy force is defined as $G = \beta g(T - \overline{T})$. Considering inclination angle, coordinate axis and gravity acceleration direction, shown in Fig. 1, all of the aforementioned relations are maintained and used except those that are modified below:

$$\tilde{f}_i(x + c_i dt, t + dt) - \tilde{f}_i(x,t) = -\frac{dt}{\tau_f + 0.5dt}\left[\tilde{f}_i - f_i^e\right]$$
$$+ \left(\frac{dt\tau_f}{\tau_f + 0.5dt}\frac{3G(c_{ix} - u)}{c^2}f_i^e\right).\sin\gamma$$
$$+ \left(\frac{dt\tau_f}{\tau_f + 0.5dt}\frac{3G(c_{iy} - v)}{c^2}f_i^e\right).\cos\gamma \tag{28}$$

According to Eq. (13), we have:

$$f_i = \frac{\tau_f \tilde{f}_i + 0.5dt f_i^e}{\tau_f + 0.5dt} + \left(\frac{0.5dt\tau_f}{\tau_f + 0.5dt}\frac{3G(c_{ix} - u)}{c^2}f_i^e\right).\sin\gamma$$
$$+ \left(\frac{0.5dt\tau_f}{\tau_f + 0.5dt}\frac{3G(c_{iy} - v)}{c^2}f_i^e\right).\cos\gamma \tag{29}$$
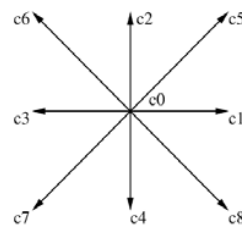

Fig. 2 Nine-speed square lattice

In this case hydrodynamic macroscopic variables are calculated as follows:

$$\rho = \sum_i \tilde{f}_i$$

$$u = (1/\rho)\sum_i \tilde{f}_i c_{ix} + \frac{dt}{2}G.\sin\gamma \qquad (30)$$

$$v = (1/\rho)\sum_i \tilde{f}_i c_{iy} + \frac{dt}{2}G.\cos\gamma$$

where $c_i = (c_{ix}, c_{iy})$ denotes discrete particle speeds.

Lid of cavity moves with velocity U_0, If H denotes cavity height, Reynolds number, Grashof number and Raleigh number are defined as $Re = U_0 H / \upsilon$, $Gr = g\beta H^3(T_h - T_c)/\upsilon^2$ and $Ra = Gr.Pr$, respectively .Characteristic dimensionless number in the analysis of mixed convection problems is Richardson number defined as $Ri = Gr / Re^2$. As stated before, lattice Boltzman method is used for near-incompressible flows; therefore, mach number is assumed as $Ma = U^* / c_s << 1$, where U^* is characteristic velocity and c_s is the lattice sound speed.

IV. BOUNDARY CONDITIONS

A. Hydrodynamic and Thermal Boundary Conditions

On the fixed walls of the cavity by using bounce back condition [2, 20-22] and on the cavity lid by equalizing density distribution function of the particle and its equilibrium state, no slip boundary condition is applied [10]. In addition, on the cavity lid and bottom wall, constant temperature condition is applied. For example, for the north wall, temperature is constant and equal as $T = T_N$, so the unknowns $\tilde{g}_4$, $\tilde{g}_8$ and $\tilde{g}_7$ are chosen as follows [2, 23]:

$$\tilde{g}_i = \rho(e_N + e') \times$$

$$\left[corresponding\ form\ for\ equilbrium \right] \qquad (31)$$

where $i = 4,8,7$

By definition:

$$\sum_i \tilde{g}_i = \rho e_N + \frac{dt}{2}\sum_i f_i Z_i \qquad (32)$$

which yields to:

$$\rho e_N + \rho e' = \frac{\rho e_N + \frac{dt}{2}\sum_i f_i Z_i - K}{\frac{1}{3} - \frac{1}{2}\frac{V_f}{c} + \frac{1}{2}\frac{V_f^2}{c^2}} \qquad (33)$$

where V_f is a flow velocity component normal to the wall, K is the sum of the six known populations, e_N denotes the imposed thermal energy density at the north wall. At the insulated walls, the constraint on the heat flux is obtained by imposing $q_x = 0$ in Eq. (25), for example for the west wall, we have [2]:

$$\sum_i c_{ix}\tilde{g}_i = 0.5dt \sum_i c_{ix} f_i Z_i + \rho e_W U_f \qquad (34)$$

The unknown populations $\tilde{g}_1$, $\tilde{g}_5$ and $\tilde{g}_8$, are chosen as

$$\tilde{g}_i = \rho(e_W + e') \times$$

$$\left[corresponding\ form\ for\ equilbrium \right] \qquad (35)$$

where $i = 1,5,8$

and become as

$$\tilde{g}_i = \left[\frac{1}{\frac{1}{3} + \frac{1}{2}\frac{U_f}{c} + \frac{1}{2}\frac{U_f^2}{c^2}} \right] \times$$

$$\left[\sum_i \tilde{g}_i + \frac{dt}{2}\sum_W \frac{c_i}{c} Z_i f_i + \rho e_W \frac{U_f}{c} \right] \times \qquad (36)$$

$$\left[corresponding\ form\ for\ equilbrium \right]$$

where $i = 1,5,8$

where U_f is a horizontal flow velocity component on the wall.

B. Macroscopic Boundary Conditions

In this work the macroscopic variables of fluid flow are made dimensionless as follows:

Dimensionless coordinates: $Y = y / H$, $X = x / H$

Dimensionless velocity components: $V = v/U_0$, $U = u/U_0$

Dimensionless temperature: $\theta = (T - T_c)/(T_h - T_c)$ (37)

Dimensionless time: $\tau = \frac{tU_0}{H}$

Therefore, dimensionless local and average Nusselt numbers along the lid and bottom wall are calculated using following relations.

$$Nu_X = -\left(\frac{\partial\theta}{\partial Y}\right)_{Y=0,1}$$
$$\qquad (38)$$
$$Nu_m = \frac{1}{AR}\int_0^{AR} Nu_X\ dX$$

In addition, dimensionless macroscopic boundary conditions are defined as follows:

$$U = V = \frac{\partial\theta}{\partial X} = 0,\quad for\ X = 0\ or\ 3;\ 0 \le Y \le 1$$

$$U = V = \theta = 0,\quad for\ Y = 0;\ 0 \le X \le 3 \qquad (39)$$

$$U = \theta = 1,\ V = 0,\quad for\ Y = 1;\ 0 \le X \le 3$$

C. Initial Conditions

The velocities of all nodes inside the cavity are taken as zero initially. The initial density is set to a value of 2.7 [10]. The initial equilibrium distribution functions are evaluated correspondingly. The initial distribution functions are taken as the corresponding equilibrium values [1].

D. Grid Independency and Validation of the Computer Program

The grid independency is studied for flow in the cavity shown in Fig. 1 for $Ri = 0.1$, $Re = 200$, $\gamma = 0^\circ$ and $Pr = 0.7$. Three grids including 300×100, 450×150 and 600×200

lattice nodes are used to perform the numerical solution. Table 1 shows the average Nu on the lid, and the values of U, V, and θ at $X = 1.5$ and $Y = 0.5$, obtained for the three different grid sizes. Due to small difference between the results of the last two grid sizes, the 450×150 grid size is chosen as a suitable one in this work.

TABLE I
AVERAGE NU ON THE LID AND U, V, θ AT $X = 1.5$ AND $Y = 0.5$

Parameters	Grid sizes		
	300×100	450×150	600×200
U	-0.197	-0.195	-0.194
V	0.063	0.066	0.067
θ	0.560	0.564	0.567
Nu_m	2.331	2.367	2.382

To validate a mixed convection problem which in ref. [25] is examined. It is a square cavity with a top lid moving with constant velocity in horizontal direction and its temperature is higher than that of the bottom wall of the enclosure. In Table 2 the average Nu on the hot wall are given for different Re and Gr. The results show good agreement with those of ref. [25].

TABLE II
AVERAGE NU ON THE HOT WALL FOR DIFFERENT RE AND GR

Re	Gr					
	10^4			10^6		
	Present work	Ref. [25]	Difference %	Present work	Ref. [25]	Difference %
400	3.55	3.62	1.97	1.17	1.22	4.27
1000	6.11	6.29	2.94	1.69	1.77	4.73

V. RESULTS AND DISCUSSIONS

In this paper, laminar flow with mixed convection heat transfer inside a two-dimensional inclined rectangular cavity with $AR = 3$ is studied numerically by using LBM for $Pr = 0.7$ and $Re = 200$ are assumed and the effects of the variations of the Ri and inclination angle on the flow and heat transfer are studied. Inclination angle varies from zero degree, horizontal cavity, to $90°$, vertical cavity. To avoid ambiguity, the cavity's walls are referred to according to the coordinates shown in Fig.1. The top lid is the hot moving wall at $Y = 1$, the bottom wall is the cold wall at $Y = 0$, and two insulated side walls are at $X = 0$ and $X = 3$. Figs. 3 and 4 show streamlines and isotherms at inclination angles $\gamma = 0, 30, 60$ and $90°$ for the cases $Ri = 0.1$ and 10. The figures show the effect of inclination angles on the flow field and heat transfer. The motion of the cavity lid causes the fluid motion in the cavity and produces a strong clockwise rotational flow in the right side of the cavity. This motion transfers hot fluid to the lower parts of the cavity, and enhances favorable pressure gradient along the vertical direction, leading to the generating buoyancy motions and transferring hot fluid from lower parts to the upper parts of the cavity. Hot fluid moves upward due to the forces resulted from the free convection in the middle and left side of the cavity. Therefore, the combination of free and forced motions, called "mixed convection", consisted of a large clockwise vortex is produced inside the cavity. In all cases, a thin hydrodynamic and thermal boundary layer is seen near the moving lid. Three regimes of the flow inside the cavity are identified corresponding to different Ri. For $Ri < 1$, forced convention, and for $Ri > 1$ free convection dominate the mechanism of heat transfer. For Ri around one, there will be mixed convection.
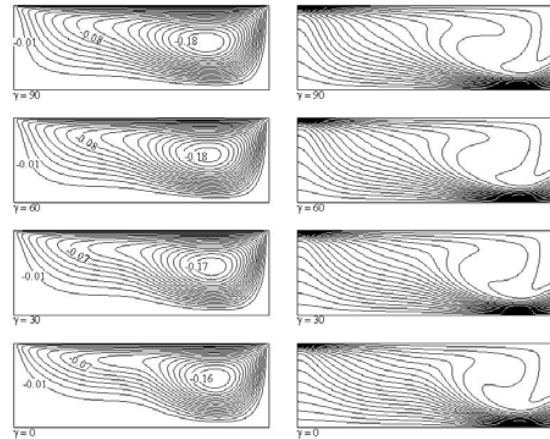

Fig 3 Streamlines and isotherms for $Ri = 0.1$, at $\gamma = 0, 30, 60$ and $90°$
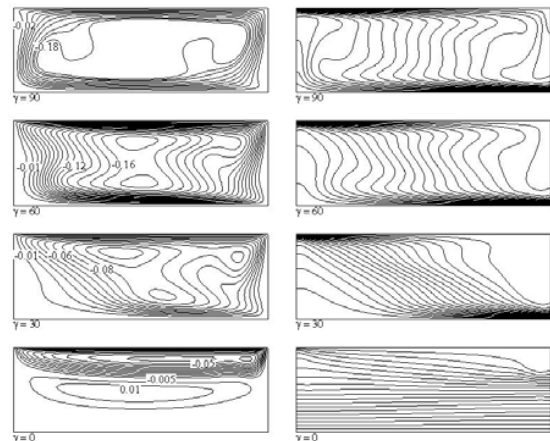

Fig. 4 Streamlines and isotherms for $Ri = 10$, at $\gamma = 0, 30, 60$ and $90°$

In Fig. 3, Ri is 0.1, so forced convection is dominant the problem. In this case a large clockwise vortex with dense lines near the moving lid affects the whole space of the cavity. The center of this vortex is located near the right wall of the cavity. In this region, fluid is pushed strongly downward. In addition, in the left side and lower parts of the cavity the rotational power and density of the streamlines of the vortex is reduced. Fig. 3 shows that by increasing the inclination angle, the rotational power of the vortex in the center of the cavity increases slightly and it does not affect significantly the other moving and thermal behavior of the fluid. By increasing the inclination angle, the rotational power of the large vortex at $Ri = 1$ increases more, compared to that at $Ri = 0.1$.
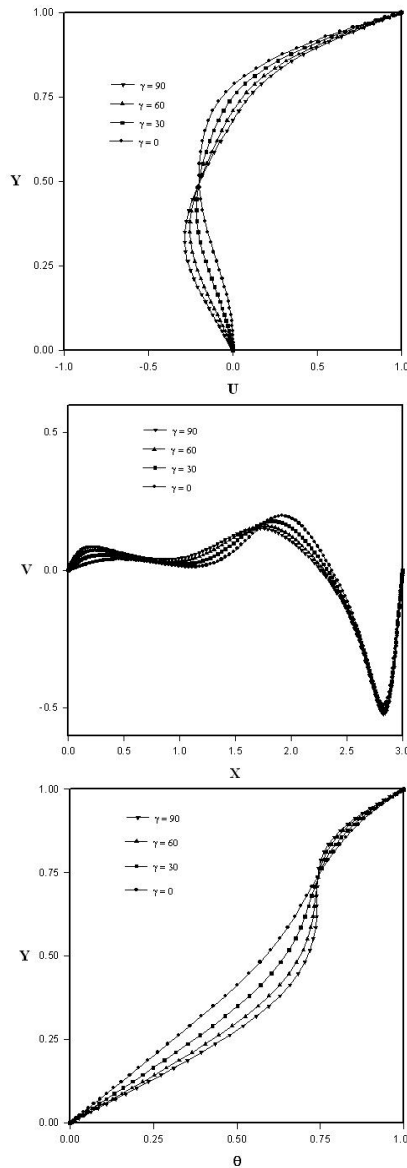
Fig. 5 U and θ along the vertical centerline and V along the
horizontal centerline for $Ri = 0.1$ at different γ

In Fig. 4, $Ri = 10$ and free convection is the main mechanism of heat transfer. In this case, the motion of the lid causes the motion of the hot fluid from upper to lower parts of the cavity, leading to a vertical favorable temperature gradient and, thus, creation of buoyancy forces. When buoyancy forces dominate the problem, inclination angle has significant effect on the flow and heat transfer, for $\gamma = 0$, isotherms in the lower half of the cavity are straight lines and perpendicular to the side walls, indicating that conduction heat transfer is dominant in this region. As inclination angle increases, the curvature of isotherms increases, indicating the enhancement of the convection. Fig. 5 shows the variations of horizontal component of dimensionless velocity, U, and temperature, θ, along the vertical centerline of the cavity; and vertical

component of dimensionless velocity, V, along the horizontal centerline of the cavity at different inclination angles for $Ri = 0.1$. It is seen that along the vertical centerline of the cavity, the component of velocity in X direction, U, is zero at $Y = 0$ and it decreases as Y increases, so that it becomes negative at $0 < Y < 0.7$. For higher values of Y, U increases and approaches to the velocity of moving lid at $Y = 1$. In addition, Fig. 5 shows that flow direction in upper part is in the same direction of the moving lid and it is opposite of the moving lid direction in the lower part of the cavity. Therefore, flow direction in the right side of the cavity must be from top to bottom. Moreover, Fig. 5 shows that along horizontal centerline of the cavity at $2.5 < X < 3$, the flow with high velocity is pushed downward, and then from middle and left side of the cavity moves upward with lower velocity. In this case, the increase of inclination angle increases the limit of U, but it does not have a significant effect on the vertical component of the velocity. It is also observed that temperature is zero at $Y = 0$ and increases strongly and linearly with Y. At $0.7 < Y < 0.8$ temperature variation is reduced, and after that it increases strongly and linearly, so that at $Y = 1$, it reaches to its maximum value. The increase of cavity inclination angle, increases the inclination of temperature profile at $0.5 < Y < 0.8$, so that at $\gamma = 90$, cavity is vertical, and in the range $0.7 < Y < 0.75$ temperature profile becomes almost a vertical line, showing no temperature variation in this case. The high variations of temperature adjacent to the moving lid and bottom wall indicate the existence of thin thermal boundary layers along these walls at $Ri = 0.1$. Figs. 6, 7 show variations of horizontal component of dimensionless velocity, U, and temperature, θ, along the vertical centerline of the cavity and vertical component of dimensionless velocity, V, along the horizontal centerline of the cavity at different inclination angles for $Ri = 1$, 10. Increasing the inclination angle from 30° to higher values, causes the increase of the absolute value of U in the lower parts of the cavity, as shown in Fig. 6. Fig. 7 shows when $\gamma = 0$, the velocity U is approximately zero in the range $0 < Y < 0.5$. Moreover, as Y increases, first it becomes negative and then it increases and approaches to its maximum value at the lid. It is observed that by increasing of the inclination angle, the velocity profile U stretches toward negative X axis in the lower parts of the cavity and toward positive X axis in the upper parts. Previous investigations have shown that in a horizontal cavity with top moving lid, the maximum value of horizontal velocity of flow is equal to the moving lid speed and occurs in the fluid adjacent to it [25, 26]. However, in this case, the increasing of the inclination angle leads to the increase of free convection heat transfer, which adds the forced motions, and thus increases the fluid U velocity to the higher value than the lid velocity.
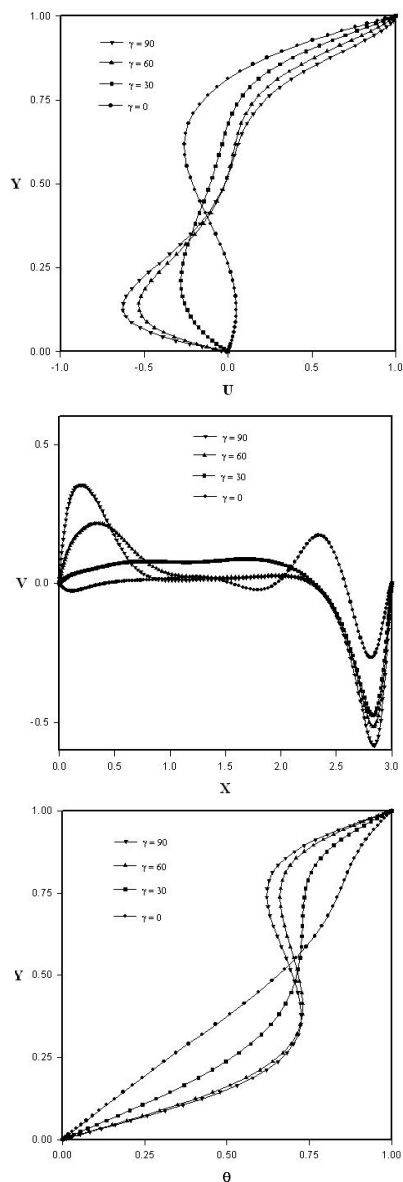
Fig. 6 U and θ along the vertical centerline and V along the horizontal centerline for $Ri = 1$ at different γ

Fig. 7 U and θ along the vertical centerline and V along the horizontal centerline for $Ri = 10$ at different γ

Fig. 8 shows the variations of average Nusselt number. It is observed that when $Ri = 0.1$, the forced convection heat transfer is dominant and Nu_m increases slightly with the increase of inclination angle. At $Ri \geq 1$, Nu_m is increased more intensively. In fact at $Ri = 10$, it is increased by a factor of 6 when inclination angle varies from 0 to $90°$, indicating that in this case free convection effect is enhanced and added to the forced convection effect. In addition, the most increasing rate of Nu_m occurs when inclination angle increases from $0°$ to $30°$ and after that the slope decreases slightly. When $\gamma = 0$, Nu_m is maximum at $Ri = 0.1$, indicating that forced convection causes maximum heat transfer in the horizontal cavity.
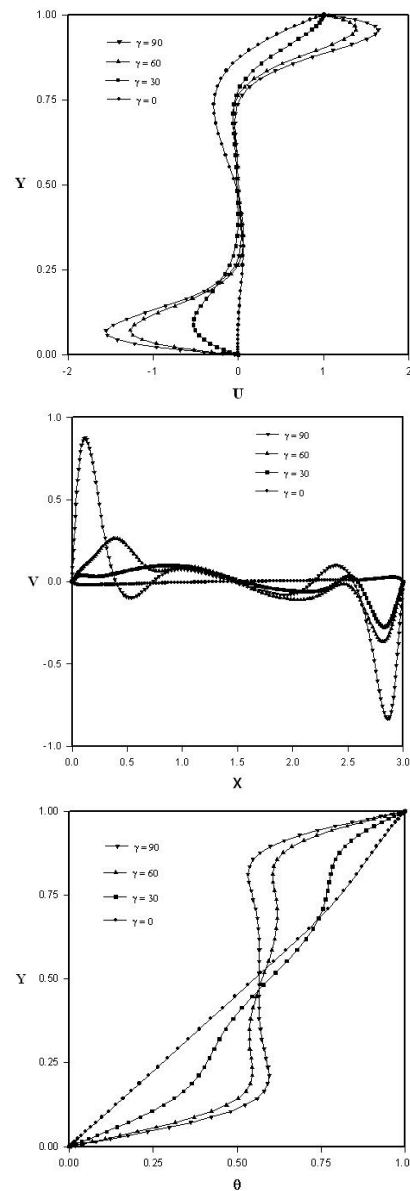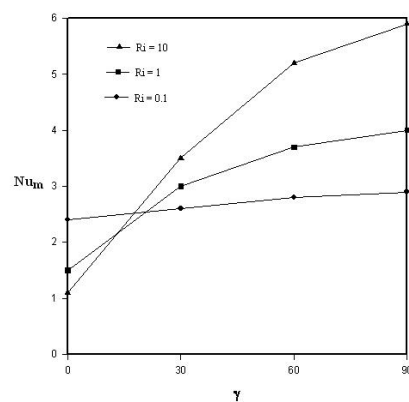

Fig. 8 Nu_m on the hot surface versus inclination angle

However, as inclination angle increases, free convection is enhanced relative to forced convection, so that for $\gamma = 30, 60, 90°$, free convection is the main factor of heat transfer and maximum Nu_m occurs at $Ri = 10$.

VII. CONCLUSION

A thermal lattice Boltzmann BGK model was used to study numerically laminar two-dimensional mixed convection heat transfer inside an inclined rectangular cavity. This method enhances the numerical stability and is able to include the viscous heating effects. The inclination of the cavity enhances the buoyancy force, which affects the velocity components of the flow. Therefore, the relations used by previous researchers to calculate collision term in the lattice Boltzmann equation and to calculate macroscopic properties of flow were modified in this paper, as shown in Eqs. (28), (29) and (30). In addition, the effects of the inclination angle of the cavity and the variations of Ri, which changes the heat transfer regimes of the flow, forced, mixed or free convection, were studied. At $Ri = 0.1$, when $\gamma = 0$ (horizontal cavity), a large and strong vortex is formed in the right side of the cavity and affects the whole flow field. In this case, by increasing the inclination angle, the rotational power of the vortex increases slightly. At $Ri = 10$, when $\gamma = 0$, a vortex affects the upper half of the cavity and another vortex affects the lower half, and when γ increases, the two vortices gradually merge, so that at $\gamma = 90$ (vertical cavity) a large, strong and symmetrical vortex affects the whole flow field. As Ri increases, free convection heat transfer is enhanced relative to forced convection. As a result, by increasing the inclination angle, the flow parameters affects more, so that at $Ri = 10$, when $\gamma = 60°$ and $\gamma = 90°$, the absolute U component of fluid velocity near the moving lid and bottom wall becomes greater than the lid velocity. At $Ri = 0.1$ (dominance of forced convection), by increasing the inclination angle, the average Nusselt number increases slightly. However, at $Ri \geq 1$, by increasing the inclination angle, Nu_m increases more intensively, so that at $Ri = 10$ (where free convection is dominant), Nu_m is increased by a factor of 6 as inclination angle is increased from 0 to 90°. It shows that the flow parameters are more sensitive to the variations of inclination angle for free convection domination case compared with the case of forced convection domination. When $\gamma = 0$, Nu_m is maximum at $Ri = 0.1$, indicating that forced convection causes maximum heat transfer in the horizontal cavity. However, as inclination angle increases, free convection is enhanced relative to forced convection, so that at $\gamma = 30, 60, 90°$, the free convection heat transfer is the main mechanism of heat transfer and maximum Nu_m occurs at $Ri = 10$. This study shows that lattice Boltzmann BGK model is capable of simulating mixed convection for wide range of flow parameters and gives reliable and accurate results.

REFERENCES

[1] Patil D.-V., Lakshmisha K.-N., Rogg B., Lattice Boltzmann simulation of lid-driven flow in deep cavities, Computers & Fluids 35 (2006) 1116-1125.

[2] D'Orazio A., Corcione M., Celata G.-P., Application to natural convection enclosed flows of a lattice Boltzmann BGK model coupled with a general purpose thermal boundary condition, Int. J. of Thermal Sciences 43 (2004) 575-586.

[3] Chen S., Doolen G., Lattice Boltzmann method for fluid flows, Annual Rev. Fluid Mech. 30 (1998) 329-364.

[4] Luo L., The lattice gas and lattice Boltzmann methods: Past, present, and future, Appl. Comput. Fluid Dyn, Beijing (2000) 52-83.

[5] Succi S., The lattice Boltzmann equation for fluid dynamics and beyond, Oxford, Oxford University Press (2001).

[6] Qian Y., Humie`res D., Lallemand P., Lattice BGK models for Navier–Stokes equation, Europhys. Lett. 17 (1992) 479-484.

[7] He X., Luo L., Theory of the lattice Boltzmann equation: From the Boltzmann equation to the lattice Boltzmann equation, Phys. Rev. 56 (1997) 6811-6817.

[8] Yu D., Mei R., Luo L., Shyy W., Viscous flow computations with the method of lattice Boltzmann equation, Progress in Aerospace Sciences 39 (2003) 329-367.

[9] Guo Zh., Shi B., Wang N., Lattice BGK model for incompressible Navier–Stokes equation, J. of Computational Physics 165 (2000) 288-306.

[10] Hou Sh., Zou Q., Chen Sh., Doolen G.-D., Cogley A.-C., Simulation of cavity flow by the lattice Boltzmann method, J. Comput. Phys. 118 (1995) 329-347.

[11] Wu J.-S., Shao Y.-L., Simulation of lid-driven cavity flows by parallel lattice Boltzmann method using multi-relaxation-time scheme, Int. J. Numer. Meth. Fluids 46 (2004) 921-937.

[12] He X., Chen Sh., Doolen G.-D., A novel thermal model for the lattice Boltzmann method in incompressible limit, J. of Computational Physics 146 (1998) 282-300.

[13] Eggels J.-G.-M., Somers J.-A., Numerical simulation of free convective flow using the lattice Boltzmann scheme, Int. J. Heat and Fluid Flow 16 (1995) 357-364.

[14] Dixit H.-N., Babu V., Simulation of high Rayleigh number natural convection in a square cavity using the lattice Boltzmann method, Int. J. of Heat and Mass Transfer 49 (2006) 727-739.

[15] Barrios G., Rechtman R., Rojas J., Tovar R., The lattice Boltzmann equation for natural convection in a two-dimensional cavity with a partially heated wall, J. Fluid Mech. 522 (2005) 91-100.

[16] Kao P.-H., Yang R.-J., Simulating oscillatory flows in Rayleigh Benard convection using the lattice Boltzmann method, Int. J. of Heat and Mass Transfer 50 (2007) 3315-3328.

[17] Bhatnagar P. L., Gross E. P., Krook M., A model for collision process in gases. I. Small amplitude processes in charged and neutral one-component system, Phys. Rev. 94 (1954) 511-1954.

[18] Cercignani C., The Boltzmann equation and its applications, Applied Mathematical Sciences, Springer-Verlag, New York 61 (1988).

[19] He X., Luo L., A priori derivation of the lattice Boltzmann equation, Phys. Rev. E 55 (6) (1997) R6333-R6336.

[20] Zou Q., He X., On pressure and velocity boundary conditions for the lattice Boltzmann BGK model, Phys. Fluids 9 (6) (1997) 1591-1596.

[21] Ziegler DP., Boundary conditions for lattice Boltzmann simulations. J. Stat. Phys. 71 (1993) 1171-1177.

[22] Ginzbourg I., Alder PM., Boundary flow condition analysis for the three-dimensional lattice Boltzmann model. J Phys. II France 4 (1994) 191-214.

[23] D'Orazio A., Succi S., Simulating two-dimensional thermal channel flows by means of a lattice Boltzmann method with new boundary conditions, Future Generation Computer Systems 20 (2004) 935-944.

[24] Kuznik F., Vareilles J., Rusaouen G., Krauss G., A double-population lattice Boltzmann method with non-uniform mesh for the simulation of natural convection in a square cavity, Int. J. of Heat and Fluid Flow 28 (2007) 862-870.

[25] Iwatsu R., Hyun J.-M., Kuwahara K., Mixed convection in a driven cavity with a stable vertical temperature gradient, Int. J. Heat Mass Transfer 36 (1993) 1601-1608.

[26] Prasad Y.-S., Das M.-K., Hopf bifurcation in mixed convection flow inside a rectangular cavity, Int. J. of Heat and Mass Transfer 50 (2007) 3583-3598.